Biotechnology Prog
DOI 10.1002/btpr.2



# Investigation of the hepatic respiration and liver zonation on rat hepatocytes using an integrated oxygen biosensor in a microscale device

Satomi Matsumoto[1,2], Astia Riski Safitri[1,3], Mathieu Danoy[3,4], Toshiro Maekawa[1,2], Haruyuki Kinoshita[1,2], Marie Shinohara[1,3], Yasuyuki Sakai[1,3], Teruo Fujii[1,2], Eric Leclerc[3,4,*]

[1] CIBiS, Center for International Research on Integrative Biomedical Systems, Institute of Industrial Science, The University of Tokyo, 4-6-1, Komaba, Meguro-ku, Tokyo 153-8505, Japan

[2] Applied microfluidic laboratory, Institute of Industrial Science, The University of Tokyo, 4-6-1, Komaba, Meguro-ku, Tokyo 153-8505, Japan

[3] Organ biosystem laboratory, Institute of Industrial Science, The University of Tokyo, 4-6-1, Komaba, Meguro-ku, Tokyo 153-8505, Japan

[4] LIMMS/CNRS-IIS (UMI 2820), Laboratory for Integrated Micro-Mechatronic Systems, Institute of Industrial Science, The University of Tokyo, 4-6-1, Komaba, Meguro-ku, Tokyo 153-8505, Japan

[*] Corresponding author



This article has been accepted for publication and undergone full peer review but has not been through the copyediting, typesetting, pagination and proofreading process, which may lead to differences between this version and the Version of Record. Please cite this article as doi: 10.1002/btpr.2854

Received: Jun 22, 2019; Revised: Jan 08, 2019; Accepted: May 15, 2019

**Abstract**

The development of an *in vitro* functional liver zonation model is a major issue to reproduce physiological liver features. Oxygen concentration is one of the potential explanations of a primary regulating factor of zonation. In this frame, we investigated the oxygen gradient inside a microfluidic device containing rat hepatocyte cultures. The device integrated a platinum (Pt) (II) octaethylporphyrin sensor, allowing a 2D mapping of the oxygen concentration. After 3h of adhesion of the hepatocytes, the sensor indicated an intense oxygen depletion, leading to an oxygen shortage in the center of the device. After a 30 min perfusion of the culture medium, we monitored the formation of the oxygen gradient along the culture due to cellular respiration. The profile of the oxygen gradient was modulated and controlled by increasing either the perfusion flow rate or the device thickness. In addition, the oxygen gradient was time dependent as far as it decreased with the time of culture. Perivenous and periportal liver patterns were characterized by the immunostaining of the hepatic markers. We put in evidence a spatio temporal hepatic organization. We observed the overexpression since 24h of perfusion of the APC and PCK1 proteins upstream in the oxygen-rich area of the device. The overexpression of GS, GCK, CYP1A, and HIF$\alpha$ proteins were observed downstream in the oxygen-poor area. Then, CYP3A2 and β-catenin spatial reorganization was achieved after 48h of culture. The results presented a partial zonation-like pattern that was superimposed with an oxygen gradient profile.

**Keywords:** oxygen sensor, hepatocyte, liver zonation



## 1 Introduction

The limited availability of functional liver models for drug testing is a major bottleneck, forcing pharmaceutical companies to spend $1 billion/year on liver cells alone[1]. Simultaneously, there are 6700 persons on the waiting list for liver organ transplantation (Journalist Workshop on Organ donation and transplantation. Recent Facts & Figures 26 November 2014 – Brussels). The future ability to produce a functional liver model will radically change this situation. To reach this goal, complex bioengineered liver organs are potential new solutions for drug testing or to model healthy and disordered livers.

Within this framework, the development of microfluidic technologies led to the achievements of various types of organ models on chips, based on the construction of microscale bioreactors[2], including liver-on-chip[3,4]. Concerning the liver, the features of those bioreactors mimic the liver physiology as much as possible. Thus, the additional integration of progress in tissue engineering [5,6], including liver cell co-cultures, three dimensional cultures, or organ-to-organ co-cultures[7,8,9] (Bauer et al., 2016; Bricks et al., 2016, Zeller et al., 2017), contribute to propose a wide range of liver-on-chip devices. The knowledge of liver organ-on-chip contributed to the proposal of even stem cell-based culture methods[10] or complex human primary cell-based models [11,12,13].

However, despite significant progress in this field of liver-on-chip, some challenges still remain. Among them, the development of an *in vitro* functional liver zonation model is a major issue to reproduce physiological liver features. In fact, along the porto-central axis of the liver lobule, hepatocytes present three different functional profiles: 1) the periportal area, specializing in glucose metabolism, 2) an intermediate area, specializing in ammonia detoxification, and 3) the perivenous area, specializing in xenobiotic detoxification [14]. Several hypotheses exist to explain this functional zonation, the common point being the existence of a gradient of concentration of soluble compounds triggering specific signaling pathways (e.g., Wnt/β-catenin and hedgehog pathways [15]). These pathways are modulated by the hypoxia signaling system, thus pointing to oxygen concentration as a potential explanation of a primary regulating factor of zonation [16,17].

Several studies presented liver zonation approaches using liver biochips [18,19]. Based on those works, the oxygen gradient in a flow chamber was correlated with the CYP450 gradient in rat hepatocytes [20,21]. In addition, few examples of devices have integrated oxygen biosensors in the liver culture chamber to couple biological and mass transport/mechanical phenomena [22,23,24]. In this view, we have proposed a technology in which an oxygen sensor layer containing Platinium (II) octaethylporphyrin (PtOEP) was embedded at the bottom of a liver-on-chip device [25]. The originality of our sensor allowed a 2D mapping of the oxygen profile and oxygen concentration over a large area (about $1cm^2$). The concentration profile was coupled with fluid dynamic and mass transport simulations. In addition, as the device is transparent, the oxygen concentration cartography could be superimposed with conventional in situ biological assays (such as immunostaining and cell tracking). The principle and the application of the device were successfully demonstrated with liver cancer line HepG2 [25]. However, HepG2 are cancerous cell lines that are reported with abnormal betacatenin regulation [26,27], which make those cells not the best model to study liver zonation. In addition, HepG2 can adapt their metabolism to hypoxia environment. In order to propose a relevant zonation tissue model, we have extended our investigation to rat primary hepatocytes. We will introduce the oxygen

sensor in the biochip and confirm the best culture condition to achieve healthy zonation-like culture with primary rat hepatocytes. Then, we will investigate the spatio-temporal oxygen profiles and the protein patterns in this new dynamic micro-environment.

## 2 Material and methods

### 2.1 Device features

The detailed fabrication process of the device is given in our previous work [25]. The concept of the device is shown in Figureure 1A. The device is composed of a hepatocyte culture chamber, which is impermeable to oxygen diffusion, but allows culture medium perfusion. Therefore, oxygen can only come from the oxygen dissolved in the culture medium. Between the inlet and outlet of the cell culture chamber, the perfusion culture creates an oxygen gradient caused by cellular respiration. Two culture chambers were tested with two heights: 300 and 500 μm. At the bottom of the chamber, there is the oxygen sensor layer. The device consists of four layers. The bottom layer is a cover glass to prevent oxygen diffusion into the device from below. The second layer is the integrated oxygen sensor embedded in a polystyrene layer made of platinum (Pt) (II) octaethylporphyrin (PtOEP), whose fluorescent intensity negatively correlates with oxygen concentration[28]. The excitation wavelength of PtOEP is 510–560 nm and the fluorescence wavelength is 650 nm [28]. The third layer is a cell culture chamber (layer made of PDMS), and the fourth layer is a top slide glass to prevent the oxygen penetration from the top. Finally, an epoxy polymer is coated around the device to ensure that the entire device is airtight and secure. The device is presented in Figures 1B to 1D.

### 2.2 Oxygen sensor calibration

We calibrated the sensor by characterizing the relationship between the fluorescence intensity of the PtOEP layer and oxygen concentration using the Stern-Volmer relationship:

(Eq. 1) $I_0/I = 1 + K_{SV}[O_2]$

where $I_0$ and $I$ are intensity values in the absence and presence of oxygen, respectively, and $K_{sv}$ is the Stern-Volmer constant. The oxygen concentration $[O_2]$ is given for a fluorescence intensity $I$ [28]. The parameters for the Stern-Volmer relationship, $I_0$ and $K_{sv}$, were determined by calibration using a commercially available optical oxygen sensor (Flow-Through Cells with Oxygen Sensor, Pyro Science, Germany). The parameters of Stern-Volmer for our devices were estimated to be $2.70 \times 10 \pm 6.15 \times 10^{-1}$ for $I_0$ and to $5.06 \times 10^{-1} \pm 2.75 \times 10^{-2}$ $mmHg^{-1}$ for $K_{sv}$. The oxygen solubility in the media 1.19 x $10^3$ pmol/mL/mm Hg was used to convert data in mmHg and mol/L [29]. To convert the unit between ppm and mol/L, we used the following equation:

(Eq. 2) $C_{(ppm)} = C_{(mg/kg)} = 10^6 \times C_{(mol/L)} \times M_{(g/mol)} / \rho_{(kg/m^3)}$

Assuming an Oxygen mass molar equal to 32 g/mol and a culture medium density equal to 1000kg/$m^3$, the equation was reduced to

(Eq. 3) $C_{(mol/L)} = C_{(ppm)} / 32\,000$

This lead to estimate a conversion rate as follow: 1ppm ≈ 31,25μmol/L ≈ 26 mmHg

**2.3 Cell culture in the device**

2.3.1 Rat hepatocytes isolation

Primary hepatocytes were isolated from an 8-weeks-old male Wistar rat (Sankyo Lab Service Corporation, Inc., Japan), using the two-step standard collagenase perfusion liver protocols as previously described[29] with a minor modification. The animal experiments were performed in accordance with the University of Tokyo guidelines for animal experiments, following the guidelines of the Japanese Ministry of Education. Shortly, after perfusion by the perfusion buffer for 8 min, the liver was disassociated by collagenase for 8–10 min. The dissociated liver was then minced, strained, collected in a tube, and centrifuged at 600 rpm for 1 min

in minimum acceleration and deceleration at 4 °C. After 3 cycles of medium washing and centrifugation at 600 rpm for 1 min 4 °C, 25 ml of hepatocyte suspension was treated with a 70 µm cell strainer (Corning Inc., USA) to remove any aggregated hepatocytes. The single hepatocyte suspension was mixed with 22.5 ml Percol (GE Healthcare, USA) and 2.5 ml HBSS 10X (Thermo Fisher Scientific K. K., USA) and the total volume was adjusted to 50 ml. Subsequently, the dead cells were removed after centrifugation at 600 rpm for 10 min at 4 °C. The hepatocyte pellet was washed with 50 ml culture medium, followed by centrifugation at 600 rpm for 1 min at 4 °C. Hepatocytes with more than 80% viability were used in the experiments. The isolated hepatocytes were cultured using William's E medium (Thermo Fisher Scientific K. K., USA) supplemented with nonessential amino acid (1%), amino acid (1%), insulin (0.1 µM), dexamethasone (1 µM), acid ascorbic (250 mM) and epithelial growth factor (EGF-20 ng/mL).

2.3.2 Rat hepatocyte cell culture in the device

The devices were washed with 70% ethanol for sterilization and treated with collagen solution. We used a Cellmatrix Type 1-P collagen (Nitta Gelatin Inc, 3.0 mg/mL). A 10% Type I-P collagen solution was prepared by mixing 1 mL of Type I-P collagen, 9 mL of MilliQ water and 10 µL of 1N HCl. The solution was incubated one hour in the device at 37 °C in a humidified atmosphere containing 5% $CO_2$ and 20% of $O_2$. The device was washed with culture medium and rat hepatocyte cells were seeded at a density of $3 \pm 1 \times 10^5$ cells/device (corresponding to $1 \times 10^5$ cells/cm$^2$) . After incubation for 3 h at 37 °C in a humidified atmosphere containing 5% $CO_2$ and 20% of $O_2$ for adhesion, the perfusion culture was initiated for 30 min at 5, 10, 15 and 20 µL/min for short-term experiments. Long-term perfusion cultures took place for 24 h and 48 h leading to 27 h and 51 h total of culture with the flow rate of 15 µL/min. Those perfusions were done also in a 5% $CO_2$ and 20% of $O_2$ incubator. The set-up is illustrated in Figureure 1E.

2.3.3 Rat hepatocyte cell cultures in Petri

Control experiments were performed in parallel of the dynamic cultures. 12 polystyrene treated-culture-well plates (1 $cm^2$, Nunc, not permeable bottom) and 12-PDMS flat-well plates (1$cm^2$, Vessel Inc., Japan, permeable bottom) were coated with the 10% Type I-P collagen for 1 h (similar preparation of section 2.3.2). The PDMS plates were used as a gas permeable plate model whereas polystyrene ones were used as non-gas permeable models. The PDMS and polystyrene plates were washed with culture medium and rat hepatocytes were seeded at a density of $1 \times 10^5$ cells/$cm^2$. Four conditions were investigated to confirm the effect of oxygen concentration on the cell adhesion and survival. To do so, the cultures were performed at 37 °C in four humidified atmospheres containing 20%, 10%, 5% and 2,5% of $O_2$ respectively.

**2.4 Fluorescent immunostaining assays**

At the end of the experiment, the biochips are assessed for the expression of liver-specific markers *via* immunostaining. We selected the albumin (ALB) because it is a marker of functional hepatocytes. HIF-1α is a marker of hypoxia. Glutamine synthetase (GS, glutamine and nitrogen metabolism), glucokinase (GCK, sugar metabolism), and cytochrome P450, family 3, subfamily a, polypeptide 2 (CYP3A2, drug metabolism) are markers of typical hepatic cellular functions, which are active in low oxygen area, while the Adenomatous Polyposis Coli (APC, “zonation keeper”) and Phosphoenolpyruvate carboxykinase 1 (PCK1, gluconeogenesis) are normally over expressed active in high oxygen area. Finally, we also targetted the betacatenin that is reported to be involved in the liver zonation formation [30].

After washing the medium with PBS (Wako 163-25265, Japan), the rat hepatocytes were fixed with paraformaldehyde (PFA) 4% (Wako 163-20145) and kept at 4 °C overnight. The next day, PFA was replaced by PBS and samples were stored at 4 °C until immunostaining.

Cells were permeabilized with Triton X100 (1/1000 in MilliQ water, plusone 17-1315-01) for 15 min at room temperature (RT) and washed with PBS. Then, samples were blocked in a gelatin solution ($Na_2HPO_4 12H_2O$, 14.5 $g.l^{-1}$ (Wako 196-02835), $NaH_2PO_4 2H_2O$, 1.48 $g.l^{-1}$ (Wako 192-02815), NaCl, 8.8 $g.l^{-1}$ (Wako 191-01665), gelatin, 1.0 $g.l^{-1}$ (Sigma 4055)) for 30 minutes at RT. Primary antibodies were incubated overnight at 4 °C in blocking buffer. The next day, secondary antibodies coupled with fluorochromes were incubated for 2 h at RT in a dark chamber. Finally, DNA was stained with DAPI (1/1000 in PBS) for 5 minutes at RT in a dark chamber. Stained tissues were kept in PBS for observation.

The observations were made immediately after staining with an Olympus IX-81 confocal laser-scanning microscope. The image processing to compare inlet and outlet signals was performed using image J. We have quantified the total fluorescent intensity in each image. DAPI values were used to normalize the measures in order to consider the local cell density into the analysis. The data were characterized by the Mann and Whitney test to compare the inlet and outlet conditions. The symbol "*" denotes that the hypothesis of equality of the two tested conditions is rejected with a risk factor of 5%.

### 2.5 Oxygen profiling methods

The oxygen concentration was determined using the KEYENCE BZ-X710 fluorescence microscope. The filter used for imaging was a KEYENCE BZ-X filter, Texas Red, for oxygen concentration. The exposure time was 0,13s.

Gnuplot was used to convert fluorescence intensity to oxygen concentration using the calibration data[25]. Gnuplot data was then post-treated in Image J software. Image J software was used to evaluate oxygen gradient slope from the 2D image of oxygen concentration using the Stern-Volner equation.

### 2.6 Oxygen consumption estimation method

We estimated that the oxygen consumption flux, OCF ($molO_2/s$), by the 1D-mass balance equation along the device's central longitudinal axis:

(Eq. 4): $(C_o - C(x))\ F = OCF$, In which

$C_0$ is the inlet concentration of dissolved oxygen, equal to 0,2 $molO_2/m^3$

C(x) is the concentration of dissolved oxygen at the "x" position of the device

F is the experimental culture medium flow rate

Assuming that all the cells are uniformly attached in the device and that they consumed uniformly the oxygen between the inlet and at the outlet of the culture chamber, we estimated that the oxygen consumption rate per cell, OCR ($molO_2/s/cell$):

(Eq. 5) $OCR = OCF/N_{cell}\ (x)$ in which $N_{cell}\ (x)$ is the cell number between the inlet and the "x" position in the device.

## 3. Results

### 3.1 Seeding and perfusion conditions

The primary rat hepatocytes were loaded onto the biochip immediately after extraction. We found that the cell adhesion occurred in the first 2 to 3 hours (Figures 2A). When the adhesion time was extended until 24 hours (without perfusion), we found that the cells died inside the biochip (data not shown). Thus, a healthy culture was not possible for long static conditions in the present biochips with rat hepatocytes. After 3 hours of adhesion, when the perfusion was set at too low a flow rate (5 μL/min and 10μL/min) or at too high a flow rate (20 μL/min in the 300 μm thick culture chamber), the cells also died or detached from the devices after 24h of perfusion. Thus, the successful hepatic culture was not possible when the perfusion lasted for 24 h in those conditions (data not shown). The optimized culture conditions were found for an adhesion period of 3 hours followed by a flow perfusion of 15

μL/min. This allowed for 24 hours and 48 hours of dynamic culture in both 300- and 500-μm thick flow chamber devices (Figures 2B to 2C).

In these culture conditions, the culture protocol was reproducible. The hepatocytes were inoculated at a cellular density close to $3 \times 10^5$ cells per device, corresponding to $1 \times 10^5$ cells/cm$^2$. The hepatocytes displayed a typical hepatic phenotype with a cuboid shape and several binucleated cells were observed. Conventional Petri control in a 20% $O_2$ incubator demonstrated successful hepatocyte adhesion after 3 hours of culture (Figureure 2D). Furthermore, after 27 and 51 hours of culture, the hepatocytes in plated cultures presented a monolayer with classical hepatocyte phenotypes (Figures 2E and 2F).

In parallel, we have investigated the effects of oxygen shortage on cellular adhesion (in polystyrene and PDMS plates) to compare with our device results. A control experiment in PDMS-plates demonstrated successful cell adhesion and healthy hepatic culture for 10%, 5% and 2.5% $O_2$ conditions after 24 hours of adhesion (Figure 3A to 3C). However, low oxygen incubator control experiments (5% and 2,5% $O_2$ conditions) have demonstrated that the hepatocytes were not able to maintain a healthy phenotype after 24 hours of culture inside the polystyrene plates (no permeable bottom) when compared PDMS-plates cultures, *i.e.*, permeable bottom (Figure 3D to 3F).

### 3.2 Oxygen gradient map during the hepatic culture

#### 3.2.1 Oxygen profiles in static conditions after the adhesion in the 300μm height chamber

During the adhesion step, before the perfusion, the large fluorescent red intensity clearly illustrated the cellular respiration and oxygen consumption during the hepatocyte adhesion (Figure 4A). Due to static cell adhesion, without flow, the intensity of fluorescence was very high in the middle of the biochip. On the inlet and

outlet sides, a weaker red intensity was observed, probably due to oxygen diffusion from inlet and outlet ports (only under static conditions at 0 μl/min, there is dead end fluid reservoirs at the inlet and outlet ports leading to this diffusion process).

The conversion using the Stern-Volmer relationship contributed to extract a measurement and a map of the oxygen concentration profile (Figure 4B). Based on the image processing done along the central axis of the biochip, we were able to extract the oxygen gradient along the device (Figure 4K). The tables 1 summarized the experimental measures. In static conditions, we measured an oxygen concentration value closed to 1 ppm (corresponding to a partial pressure of 26 mmHg and 31,25μmol/L) in the center of the device (Figure 4K). This result demonstrated that the cellular respiration induced an oxygen shortage after 3 hours of adhesion. This oxygen shortage was measured starting at 8 mm from the inlet. This led to estimate a gradient of approximately 0.75 ppm/mm (23,4μmol/L/mm and 19,5 mmHg/mm).

### 3.2.2 Oxygen profiles after 30min of perfusion after the adhesion in the 300μm height chamber

After 3 hours of adhesion, we have tested the effect of a short-term perfusion (30min) on the oxygen profiles using five flow rate conditions: 0, 5, 10, 15 and 20 μL/min (Figure 4). These tests have illustrated the cellular respiration in the biochip by the depletion of the oxygen provided by the culture medium thanks to perfusion. Thus, by increasing the flow rate, several profiles of the oxygen gradient in the biochip were monitored. The oxygen concentration profile was modified and characterized by an oxygen shortage moving downstream of the culture chamber as

the flow rate increased. This was illustrated by a red fluorescence appearing closer to the outlet when the flow rate increased (Figure 4C to 4J).

After 30 min of perfusion, at 5 and 10 μL/min, the flow did not contribute to reduce the oxygen shortage when compared to static conditions. Those culture conditions still lead to a create a sharp oxygen gradient in the 300 μm height culture chamber device (Figure 4K, table 1). In the perfusion experiments at 15 and 20 μL/min, we observed the formation of a weaker oxygen gradient. The quantity of oxygen provided by the medium at those flow rates contributed to the decrease of the absolute maximal value of oxygen depletion in the center of the biochip (table 1, Figure 4K). Thus, at 15 μL/min, we estimated a gradient closer to 0.41 ppm/mm (12,8 μmol/L/mm and 10,7 mmHg/mm). At 20 μL/min, a low oxygen depletion with a high concentration of oxygen equal to 4 ppm (125μmol/L and 114,7mmHg partial pressure) was measured at the center of the device. The gradient was estimated to be 0.2 ppm/mm (6,3 μmol/L/mm and 5,2 mmHg/mm).

Based on the values of the measured oxygen concentrations in biochip and the estimation of the cell numbers in the culture chamber ($3x10^5$ cells/device), we could extract an estimation of the oxygen consumption rate of the hepatocyte closed to $2.6 \times 10^{-16}$ mol$O_2$/s/cell.

### 3.2.3 Oxygen profiles after 24h and 48h of perfusion after the adhesion in the 300μm height chamber

Then, the characterization of the oxygen concentration and the typical profiles were analyzed in the optimized 15μL/min flow rate condition after 24h and 48h of perfusion (*n.b.* the hepatocytes died in the other conditions after 24h of perfusion).

We found that the gradient was weaker after 24 h of perfusion when compared to the ones measured after 3 h of adhesion followed by 30 min of perfusion (Figure 4L). In the 300 μm height flow chamber devices, the gradient was estimated to be 0.27 ppm/mm (8,3 μmol/L/mm and 7 mmHg/mm) after 24h of perfusion (table 1). As the gradient was weaker when compared to the 30 min perfusion after the adhesion step, it also resulted in a smaller oxygen consumption rate. Based on those experiments, we estimated that the hepatocyte oxygen consumption rate was closed to $2.1 \pm 0.1 \times 10^{-16}$ mol$O_2$/s/cell after 24 h of perfusion.

After 48h of perfusion, the gradient was still observed but became milder than after 24h of perfusion. We estimated a value equal to 0,13ppm/mm (4.1μmol/L/mm and 3,4 mmHg/mm). As a result, the oxygen consumption in the device was also lower than the consumption monitored at 24h of perfusion. At 15μL/min, this led to estimate an oxygen consumption rate of $1,0 \pm 0.05 \times 10^{-16}$ mol$O_2$/s/cell after 48h of perfusion.

### 3.2.3 Oxygen profiles in the 500μm height chamber

The 500 μm height culture chamber modified the oxygen gradient when compared to the 300μm ones. The higher culture chamber device led to the creation of less sharp gradients (Figure 5). After 30 min of perfusion (after the 3h of adhesion), at 0 and 5 μL/min, both profiles superimposed, and the oxygen shortage occurred at 13 mm from the inlet (table 1, Figure 5A). This led to an estimated gradient value close to 0.54 ppm/mm (17 μmol/L/mm and 14 mmHg/mm). Then, the oxygen profiles clearly showed that, at 10 to 20 μL/min, the tissue was oxygenated up to the middle of the device. Nevertheless, at 10 μL/min, we still observed a full oxygen depletion in the after the center of the device. The oxygen concentration in the center of the biochip was measured to be 1 ppm (31,25 μmol/L and 26 mmHg partial pressure) at 10 μL/min

At 15 and 20 µL/min, the oxygen profiles superimposed and illustrated oxygenation gradients all along the entire device. The oxygen concentration in the center of the biochip was measured to be closed to 4.5 ppm (140 µmol/L and 117 mmHg partial pressure, table 1, Figure 5A).

The gradients were estimated equal to 0.46 ppm/mm (26 µmol/L/mm and 12 mmHg/mm); 0.26 ppm/mm (8,1 µmol/L/mm and 6,8 mmHg/mm) and 0.23 ppm/mm (7,2 µmol/L/mm and 6 mmHg/mm) at 10, 15 and 20 µL/min respectively.

After 24h of perfusion at 15 µL/min, the oxygen gradient was reduced when compared to the post adhesion situation (Figure 5B), similarly to the observation made in the 300µm height culture chamber. The gradient was estimated to be 0.13 ppm/mm (4,2 µmol/L/mm and 3,4 mmHg/mm) in the 500µm height flow chamber devices (table 1).

### 3.3 Functional gradient in liver biochip

We have investigated the expression of specific liver proteins in the biochips after 3 h of adhesion followed by 24 h and 48 h of perfusion at 15µL/min. Two areas of the biochips, corresponding to two oxygen concentrations, were compared. The first area was located close to the inlet, whereas the second one was located close to the outlet.

Typical results are presented in Figure 6 and Figure 7 for several devices after 24h of perfusion in the 300 µm height flow chamber device. The results revealed higher fluorescence levels of HIFα, GS, GCK, CYP1A1 (n=3 biochips) at the outlet of the biochips, corresponding to the low oxygen area conditions. Conversely, higher fluorescence levels were observed in rat hepatocytes for APC and PCK1 proteins at the inlet of the biochips, in the area corresponding to high oxygen conditions (n=3 biochips). Additional results revealed that the β-catenin protein was overexpressed at

the outlet or at the inlet according to the devices. Both albumin and CYP3A2 proteins were not differentially expressed at the inlet and outlet.

Using the 500μm height flow chamber device, we were not able to visualize specific functional gradient (data not shown) after 24h of perfusion. As a result, we extended the perfusion culture over 48h of perfusion only in the 300 μm height flow chamber device and to check the zonation marker in those devices. After 48h, the CYP3A2 and ALB become clearly over expressed at the outlet of the devices, as illustrated in the Figures 7 and 8. In addition, the β-catenin became over expressed in the inlet of the device, in the area of high oxygen concentration. Furthermore, when compared to 24h of perfusion, the β-catenin accumulated in the nucleus. This accumulation was more largely observed in the outlet than in the intlet (Figure 8). Finally, other markers such as GS, GCK, PCK1, HIF, APC remained also differentially over expressed between the inlet and outlet as they were after 24h of perfusion.

## 4 Discussion

Reproduction of the liver zonation *in vitro* is a key issue of pertinent functional hepatic models. Several *in vitro* cultures using bioreactors have been reproduced successfully with a nutrient gradient on hepatocyte cultures and various chemical and xenobiotics gradients to investigate the liver zonation [31]. In the present work, we have incorporated an oxygen sensor to enhance the technological features of the *in vitro* models. Based on our oxygen sensor integration, we observed the oxygen gradient along the cell culture generated by cellular respiration. Furthermore, we were able to superimpose oxygen-sensing data with an immunostaining dataset of functional liver markers. Finally, we were able to extract the estimations of the oxygen consumption along the device.

The oxygen sensor demonstrated the cellular hepatic respiration in the biochip. Due to the impermeable characteristic of this device, a lack of oxygen

occurred rapidly inside the chamber. This led to difficult static culture conditions after 3 h of adhesion, when compared to previous rat hepatocyte cultures performed in PDMS devices, in which overnight static cell adhesion processes were successful [3, 32] . Thus, the choice of the flow rate and the time to start the dynamic culture appeared to be critical parameters. Too high flow rate, at 20 μL/min in the 300 μm height flow chamber device, leading to a shear stress value, $\tau$ , of $1.6 \times 10^{-3}$ Pa, did not permit the maintenance of a healthy culture condition (estimated using conventional parallel plate flow chamber equation, $\tau = \mu Q/(wh^2)$ in which *Q* is the flow rate, *w* is the device width (11 mm), *h* is the device height (300 μm) and $\mu$ is the viscosity ($1.1 \times 10^{-3}$ Pa.s)). This value of critical flow rate was lower than what was previously reported with rat hepatocyte biochips, in which flow rates up to 40 μL/min (with shear stress up to $4.5 \times 10^{-3}$ Pa) were successfully used for 96 h of culture perfusion[3]. In parallel, too low flow rates contributed to provide a too low quantity of oxygen to the rat hepatocytes, also leading to their deaths. The additional petri experiments in low oxygen conditions also prove the difficulty of healthy culture under too important *in vitro* hypoxia conditions (Figure 3). Based on our protocol, we found that a flow rate of 15 μL/min resulted to a stable culture condition. This condition led to an oxygen input of $3 \times 10^{-9}$ mol$O_2$/s and a shear stress limit of $1.2 \times 10^{-3}$ Pa, for successful hepatocyte cultures. This shear stress value is lower than the physiological value of shear stress in hepatic sinusoid $9.7 \times 10^{-1}$ Pa [33]. This high hepatic shear stress is measured *in vivo* in blood capillaries composed of endothelial cells that are not involved in our present model. Therefore, a relevant co-culture with liver sinusoidal cells would be required to enhance the physiology of our tissue model.

Literature reports primary hepatocyte oxygen consumption ranging from 3 to 9 $10^{-16}$ mol$O_2$/s/cell in pig [34] and $4 \times 10^{-16}$ mol$O_2$/s/cell in rat [35,21]. In the present culture format, the consumption of oxygen by the rat hepatocytes measured after the adhesion step was estimated about $2.6 \times 10^{-16}$ mol$O_2$/s/cell. Our rat oxygen

consumption estimated value appeared in the same range but was nevertheless lower than those literature data. Although we did not identify the reason of this difference, several hypotheses can be formulated such as the levels of the sensors sensibilities, some device imperfection (residual oxygen leakage through PDMS due to unperfect hermetic closure) or hepatocytes protocol preparation (type of rats, cell isolation and culture modes). In addition, the oxygen available in static conditions, either in 300 or 500 μm height flow chamber devices, contributed to provide a critically low amount of oxygen to the hepatocytes during the adhesion step. In fact, we estimated that a cell type requiring only $0.5 – 1 \times 10^{-17}$ mol$O_2$/s/cell could be able to attach in the present device (based on the dissolved quantity of oxygen inside the culture medium remaining at rest in the device during the adhesion step). In addition, the adhesion phase probably required a lot of oxygen and energy. This phenomenon was also observed in the PDMS biochip culture with HepG2 cells in which a high energy request, *via* a high glucose consumption, was monitored in the first hours of culture[36]. As a result, the balance between the time for cell attachment and the flow required to provide oxygen in sufficient amount and with an appropriately low shear stress (to avoid cell detachment) was a key adjustment to successfully use our new device.

In the 15μL/min flow condition, the oxygen gradient was estimated to be 0.41 and 0.27 ppm/mm in 300μm and 500μm height flow chamber devices after the 3 h of adhesion, respectively. This gradient led to partial pressures ranging from 200 mmHg in the inlet and close to few mmHg in the outlet in the early time of the perfusion after the adhesion. However, after the 24 h and 48 h of perfusion, we measured weaker oxygen gradients and cell oxygen consumption rates. The reduction of oxygen consumptions in hepatocyte long-term cultures were already reported in rat and porcine primary cells[34,35]. Our results appeared in agreement with those observations. Nevertheless, a longer-term experiment (up to one week) would be necessary to confirm how would stabilize the oxygen concentration and respiration in the present biochip.

*In vivo*, the oxygen concentration gradient contributes to create oxygen-rich areas with a partial pressure of 60–65 mmHg in the periportal zone and oxygen-poor areas with a partial pressure of 30–35 mmHg in the perivenous zone. We were not able to completely reproduce this gradient. In fact, in the incubator, the culture medium is entering the biochip with a partial pressure close to 200 mmHg, which contributes to an over-oxygenated condition. In addition, at 15 μL/min, at the outlet of the device, we measured a value of oxygen concentration closed to 10 mmHg (after 30min of perfusion) and closed to 100 mmHg (after 48h of perfusion). As a result, the physiological area in the biochip is limited, both in time and in space to a specific part of the device. Thus, to be able to move to a more relevant gradient, the oxygen partial pressure needs to be equilibrated before the culture medium arrives to the cells (by integrating gas exchange module prior the cell culture chamber for instance).

The oxygen gradient is thought to be one of the causes of heterogeneity in hepatocytes' functions, depending on the positions in the liver[16]. This heterogeneity is called liver zonation. That is one reason why several approaches to build functional bioartificial livers are trying to take into account zonation-like patterns[37]. *In vivo*, it is reported that gluconeogenesis, urea synthesis, and fatty acid β oxidization are mainly taking place in the periportal zone of the lobule, where the concentration of oxygen is high. Detoxification processes (such as drug metabolism), glycolysis signaling, and alcohol metabolism are reportedly processed in the perivenous part of the lobule, which is in a hypoxic state. Therefore, reproducing this liver oxygen gradient in an *in vitro* device would provide a useful physiological liver model. In our work, typical periportal markers such as PCK1 and APC were overexpressed at the entrance of the biochip, where the oxygen concentration was the highest in the biochip after 24 h of perfusion. Simultaneously, perivenous markers, such as HIF, GS, GCK, and CYP1A1, were overexpressed in the low oxygen concentration area since 24 h of perfusion. We observed a clear CYP3A2 and β-catenin spatial specific expression in

our device after 48 h of perfusion. The CYP3A2 spatial distribution in a flow chamber with rat hepatocytes has been mapped along an oxygen gradient after 5 days of culture [21] . Similarly, the expression of our selected set of markers contributed to show a partial zonation-like behavior after 48 h of perfusion. Furthermore, nucleus accumulation at the outlet of the device, after 48h of culture was consistent with literature report of β-catenin accumulation in the nucleus of hepatocytes in the pericentral vein (low oxygen area [38]). However longer culture experiments will be required to confirm these results regarding the oxygen profile evolution that we monitored (lower gradient with time) because of the modulation of the oxygen gradient in our experiment when culture time increased. Additional analysis in our device, including zonation markers and functional assays (such as CYP3A2 metabolism assays, β-catenin signaling), will be necessary, especially on longer-term experiments to confirm if our zonation profile can be enhanced and functional.

## Conclusions

We have proposed a rat hepatocyte culture protocol in a microscale device with an integrated oxygen sensor. The sensor was able to monitor the hepatocytes' respiration. The oxygen concentration gradient was measured during the hepatocyte culture. The oxygen consumption rate displayed a reduction of the oxygen consumption between the cell adhesion phase, 24 h and 48 h of perfusion. Functional zonation markers were specifically spatially expressed along the device. This led to the achievement of a partial liver-like zonation in the device after 48h of culture. The device showed that it successfully allowed the experimental analysis of liver-specific functions in correlation with oxygen profiles.

## Acknowledgments

This work was supported by JST, CREST (JPMJCR12W3), Japan. We thank the ANR support *via* the Ilite project ANR-16-RHUS-0005, France. We also thank the LIMMS for its internal 2017 funding.

## 5 References

1 Nahmias Y., Scientists create functional liver cells from stem cells: Major implications for liver biology, drug discovery. ScienceDaily. ScienceDaily, 30 July, 2015

2 Capulli, A. K. et al. Approaching the in vitro clinical trial: engineering organs on chips. Lab Chip 14, 3181–3186 , 2014.

3 Baudoin R, Alberto G, Legendre A, Paullier P, Naudot M, Fleury M, Jacques S, Griscom L, Leclerc E, Investigation of the levels of expression and activity of detoxication genes of primary rat hepatocytes under various flow rates and cell densities in microfluidic biochips, Biotechnology Progress, Vol.30, pp.401-410, 2014

4 Sivaraman A, Leach JK, Townsend S, Iida T, Hogan BJ, Stolz DB, Fry R, Samson LD, Tannenbaum SR and Griffith LG, A Microscale In Vitro Physiological Model of the Liver: Predictive Screens for Drug Metabolism and Enzyme Induction. Current Drug Metabolism. 6:569-592, 2005.

5 Guguen-Guillouzo C, Guillouzo A., General Review on In Vitro Hepatocyte Models and Their Applications. In Hepatocytes; Methods in Molecular Biology; Humana Press: Totowa, NJ, USA, 640: 1–40, 2010.

6 Bhatia, S. N., Underhill, G. H., Zaret, K. S. & Fox, I. J. Cell and tissue engineering for liver disease. Sci. Transl. Med. 6, 245sr2-245sr2 , 2014.

7 Zeller P, Legendre A, Jacques S, Fleury MJ, Gilard F, Tcherkez G, Leclerc E, Hepatocyte-Sertoli cells coculture in bioreactor improves the Sertoli barrier permeability, Journal of Applied toxicology, 37, 287-295, 2017

8 Bricks T, Hamon J, Fleury M-J, Jellali R, Merlier F, Herpe Y-E, Seyer A, Regimbeau J-M, Bois F-Y, Leclerc E, Investigation of omeprazole and phenacetin

first-pass metabolism in humans using a microscale bioreactor and pharmacokinetic models, Biopharm Drugs Dispo, 36, 275-293, 2015

9 Bauer S, Wennberg Huldt C, Kanebratt KP, Durieux I, Gunne D, Andersson S, Ewart L, Haynes WG, Maschmeyer I, Winter A, Ämmälä C, Marx U, Andersson TB. Functional coupling of human pancreatic islets and liver spheroids on-a-chip: Towards a novel human ex vivo type 2 diabetes model, Sci Rep. , 8:1672, 2018

10 Giobbe G, Michielin F, Luni C, Giulitti S, Martewicz S, Dupont S, Floreani A and Elvassore N, Functional differentiation of human pluripotent stem cells on a chip Nature methods, 12 : 637-643, 2015

11 Novik E, Maguire TJ, Chao P, Cheng KC, Yarmush ML, A microfluidic hepatic coculture platform for cell-based drug metabolism studies, Biochemical Pharmacology.79, 1036-1044, 2010.

12 Jellali, R., Bricks, T., Jacques, S., Fleury, M.J., Paullier, P., Merlier, F., Leclerc, E., Long term human primary hepatocyte cultures in a microfluidic liver biochip show maintenance of mRNA levels and higher drugs metabolisms when compared to Petri cultures. Biopharm. Drug Dispos. 37, 264-275, 2016.

13 Chao P, Maguire T, Novik E, Cheng KC and Yarmush ML, Evaluation of a microfluidic based cell culture platform with primary human hepatocytes for the prediction of hepatic clearance in human, Biochemical pharmacology. 78, 625-632, 2009.

14 Soto-Gutierrez A, Gough A, Vernetti L, Taylor , DMonga S, Pre-clinical and clinical investigations of metabolic zonation in liver diseases: The potential of microphysiology systems, Experimental Biology and Medicine; 0: 1–12, 2017

15 Torre C, Perret C, Colnot S, Transcription dynamics in a physiological process: β-catenin signaling directs liver metabolic zonation, The International Journal of Biochemistry and Cell Biology, 43, 271-278, 2011.

16 Jungermann K, T. Kietzmann T, Oxygen: modulator of metabolic zonation and disease of the liver, Hepatology, 31, 255-260, 2003.

17 Kietzmann, T. Metabolic zonation of the liver: The oxygen gradient revisited. Redox Biol. 11, 622–630 , 2017.

18 Tiles A, Baskaran H, Roy P, Yarmush M, Toner M, Effects of oxygenation and flow on the viability and function of rat hepatocytes cocultured in a microchannel flat-plate bioreactor, Biotechnlogy and Bioengineering, 73, 379-389. 2015.

19 Foy B, Rotem A, Toner M, Tompkins R, Yarmush M: A device to measure the oxygen uptake rate of attached cells: importance in bioartificial organ design, Cell Transplantation, 6, 515-527, 1994.

20 Allen J, Bhatia S, Formation of steady-state oxygen gradients in vitro: application to liver zonation, Biotechnology and Bioengineering, 82, 253-262, 2003.

21 Allen, J. W., Khetani, S. R. & Bhatia, S. N. In Vitro Zonation and Toxicity in a Hepatocyte Bioreactor. Toxicol. Sci. 84, 110–119, 2005.

22 Bavli D, Prill S, Ezra E, Levy G, Cohen M, Vinken V,m Vanfle J, Jaeger M, Nahmias Y, Real-time monitoring of metabolic function in liver-on- chip microdevices tracks the dynamics of mitochondrial dysfunction, PNAS, 2016, 113 : E2231‑E2240

23 Moya A, Ortega-Ribera M, Guimerà X, Sowade E, Zea M, Illa X, Ramon E, Villa R, Gracia-Sancho J and Gabriel G, Online oxygen monitoring using integrated inkjetprinted sensors in a liver-on-a-chip system, Lab Chip,, 18, 2023, 2018

24 Sato A, Kadokura K, Uchida H, Tsukada K, An in vitro hepatic zonation model with a continuous oxygen gradient in a microdevice, Biochemical and Biophysical Research Communications, 453, 767-771, 2014.

25 Matsumoto S , Leclerc E, Maekawa T, Kinoshita H, Shinohara M, Komori K, Sakai Y, Fujii T, Integration of an Oxygen Sensor for Gradient Characterization in a PDMS Hepatocyte Culture Device, Sensors and actuators, 273, 1062-1069, 2018

26 Carotenuto P, Fassan M, Pandolfo R, Lampis A, Vicentini C, Cascione L, Paulus-Hock V, Boulter L, Guest R, Quagliata L, Hahne JC, Ridgway R, Jamieson T, Athineos D, Veronese A, Visone R, Murgia C, Ferrari G, Guzzardo V, Evans TRJ, MacLeod M, Feng GJ, Dale T, Negrini M, Forbes SJ, Terracciano L, Scarpa A, Patel T, Valeri N, Workman P, Sansom O, Braconi C. Wnt signalling modulates transcribed-ultraconserved regions in hepatobiliary cancers. *Gut*, 66:1268-1277, 2017

27 Lachenmayer *A,* Alsinet C, Savic R, Cabellos L, Toffanin S, Hoshida Y, Villanueva A, Minguez B, Newell P, Tsai HW, Barretina J, Thung S, Ward SC, Bruix J, Mazzaferro V, Schwartz M, Friedman SL, Llovet JM, Wnt-pathway activation in two molecular classes of hepatocellular carcinoma and experimental modulation by sorafenib. *Clin. Cancer Res.* 18:4997–5007, 2012.

28 Montagne K, Komori K, Yang F, Tatsuma T, Fujii T, Sakai Y: A micropatterned cell arraywith an integrated oxygen-sensitive fluorescent membrane, Photochemical and Photobiological Sciences, 8,1529-1533, 2009.

29 Xiao, W. Perry, G. Komori, K. and Sakai, Y. New physiologically-relevant liver tissue model based on hierarchically cocultured primary rat hepatocytes with liver endothelial cells. Integrative Biology 7, 1412-1422, 2015.

30 Behari J, The Wnt/β-catenin signaling pathway in liver biology and disease, Expert Rev Gastroenterol Hepatol. 2010; 4: 745–756.

31 Ebrahimkhani M, Shepard Neiman J, Raredon M, D,Griffith L, Bioreactor Technologies to Support Liver Function In Vitro, Adv Drug Deliv Rev. 2014 Apr; 0: 132–157.

32 Legendre A, Jacques S, Dumont F, Cotton J, Paullier P, Fleury MJ, and Leclerc E, Investigation of the hepatotoxicity of flutamide: pro-survival/apoptotic and necrotic switch in primary rat hepatocytes characterized by metabolic and transcriptomic profiles in microfluidic liver biochips, Toxicology in vitro, 28, 1075–1087, 2014

33 Puhl G, Schaser, Vollmar B, Menger M.D, Settmacher U, Noninvasive *in vivo* analysis of the human hepatic microcirculation using orthogonal polarization spectral imaging," Transplantation, 75, 756-761, 2003.

34 Balis UJ, Behnia K, Dwarakanath B, Bhatia SN, Sullivan SJ, Yarmush ML, Toner M., Oxygen consumption characteristics of porcine hepatocytes, Metab Eng.1, 49-62, 1999.

35 Rotem A, Toner M, Tompkins R, Yarmush M: Oxygen uptake rates in cultured rat hepatocytes, Biotechnology and Bioengineering, 40, 1286-1291, 1992.

36 Prot JM, Aninat C, Griscom L, Razan F, Brochot C, Guillouzo C, Legallais C, Corlu A, Leclerc E. Improvement of HepG2/C3a cell functions in a microfluidic biochip. Biotechnol. Bioeng., 108, 1704–1715, 2011.
37 Davidson A J, Ellis M J, Chaudhuri J B, A theoretical approach to zonation in a bioartificial liver," Biotechnology and Bioengineering, 109, 234-243, 2012.
38 Pal Monga S, *β*-Catenin Signaling and Roles in Liver Homeostasis, Injury, and Tumorigenesis, Gastroenterology. 148, 1294–1310, 2015.

Table 1: Oxygen concentrations and gradients in the 300 and 500μm height flow chambers for various flow rates and time of perfusion.

| Flow rates (μL/min) | Concentration in the center of device (ppm) | Abscise used to calculate the gradient (mm) | Gradient (ppm/mm) | Flow chamber height (μm) | Time of perfusion (hours) |
|---|---|---|---|---|---|
| 0 | 1 | 8* | 0,75 | 300 | 0,5 |
| 5 | 1 | 8* | 0,75 | 300 | 0,5 |
| 10 | 1 | 9* | 0,66 | 300 | 0,5 |
| 15 | 2 | 12* | 0,41 | 300 | 0,5 |
| 20 | 4 | 15** | 0,2 | 300 | 0,5 |
| 15 | 4 | 15** | 0,27 | 300 | 24 |
| 15 | 6 | 15** | 0,13 | 300 | 48 |
| 0 | 1 | 13* | 0,54 | 500 | 0,5 |
| 5 | 1 | 13* | 0,54 | 500 | 0,5 |
| 10 | 1 | 15** | 0,46 | 500 | 0,5 |
| 15 | 4 | 15** | 0,27 | 500 | 0,5 |
| 20 | 4,5 | 15 ** | 0,23 | 500 | 0,5 |
| 15 | 6 | 15 ** | 0,13 | 500 | 24 |

*correspond to the location where the minimum value of oxygen is reached; ** center of the device; 1ppm=31,25μmol/L =26mmHg

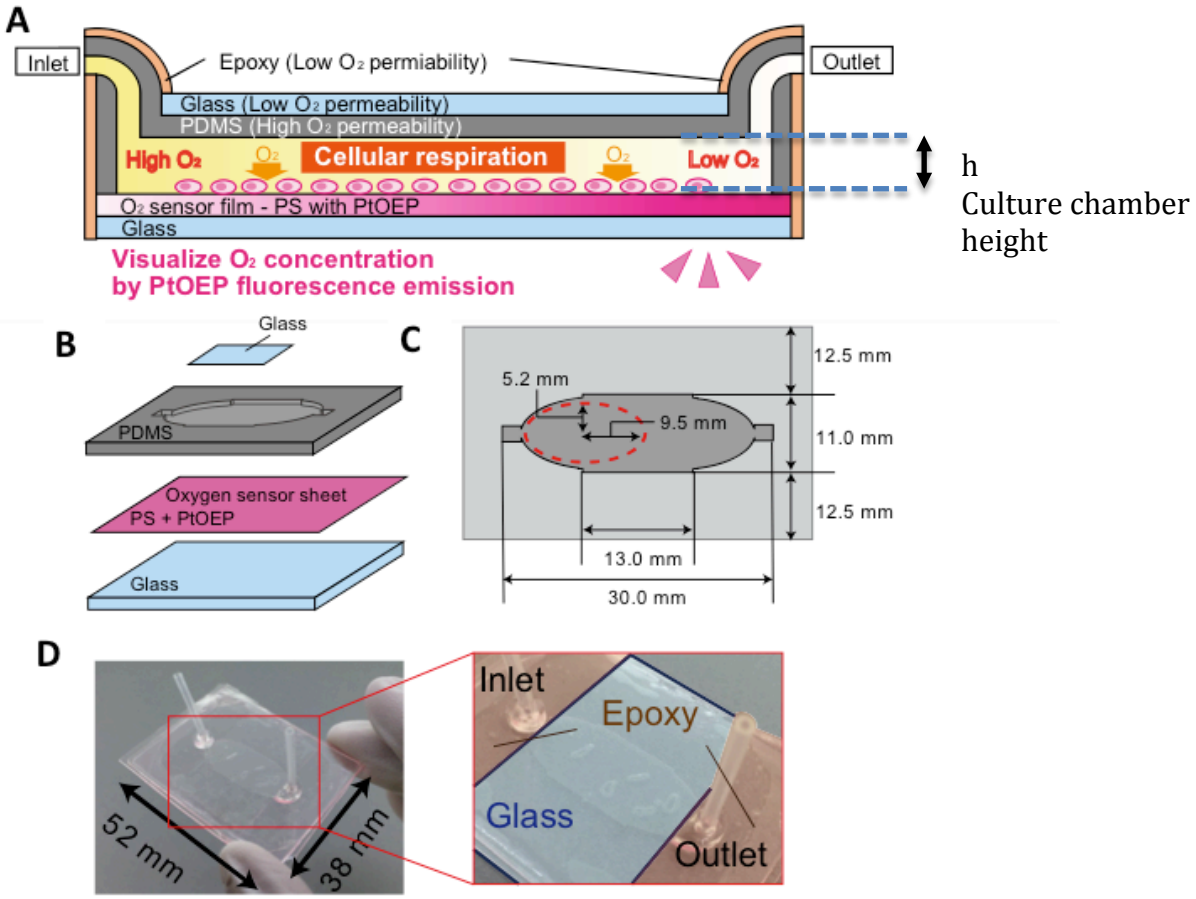

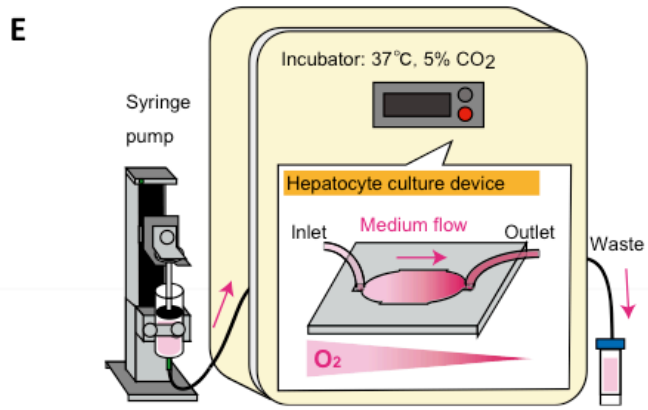


**Figure 1:** Device concept, geometrical characteristics and perfusion set up

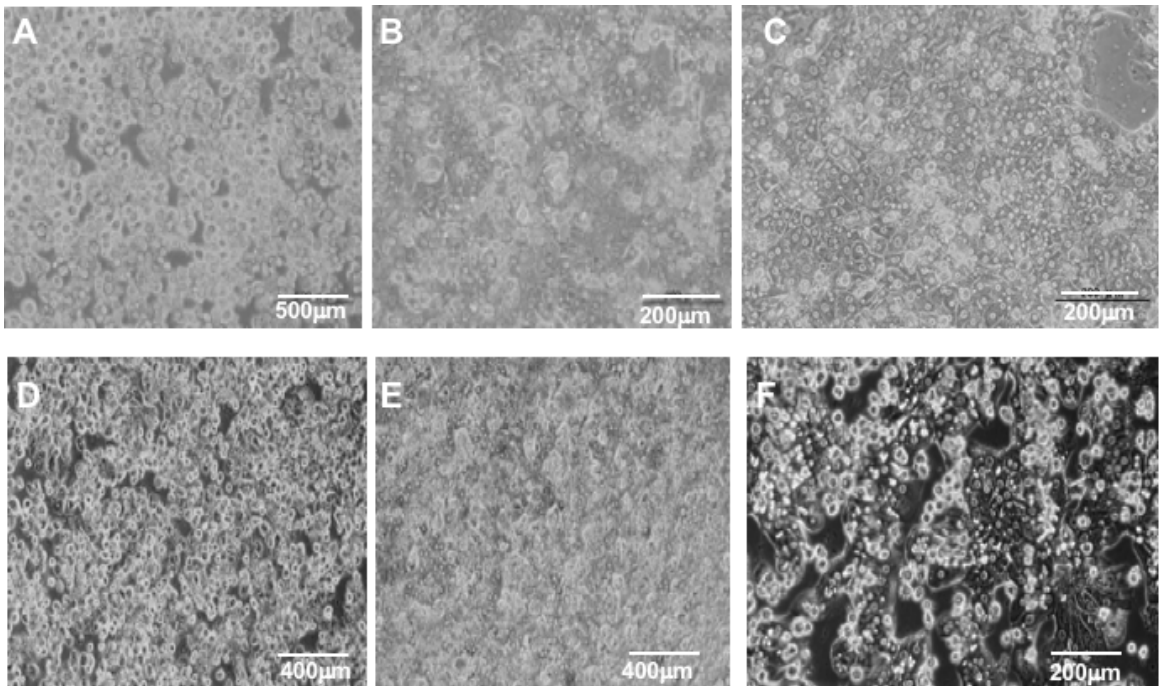


**Figure 2:** Rat hepatocyte morphologies in biochips after 3h at rest for adhesion (A) 3h at rest followed by 24h of perfusion at 15µL/min (B); 3h at rest followed by 48h of perfusion at 15µL/min (C); control hepatocytes in Petri after 3h (D) after 27h (E) and 48h (F) of culture. The cultures are performed in a 20% $0_2$ incubators.

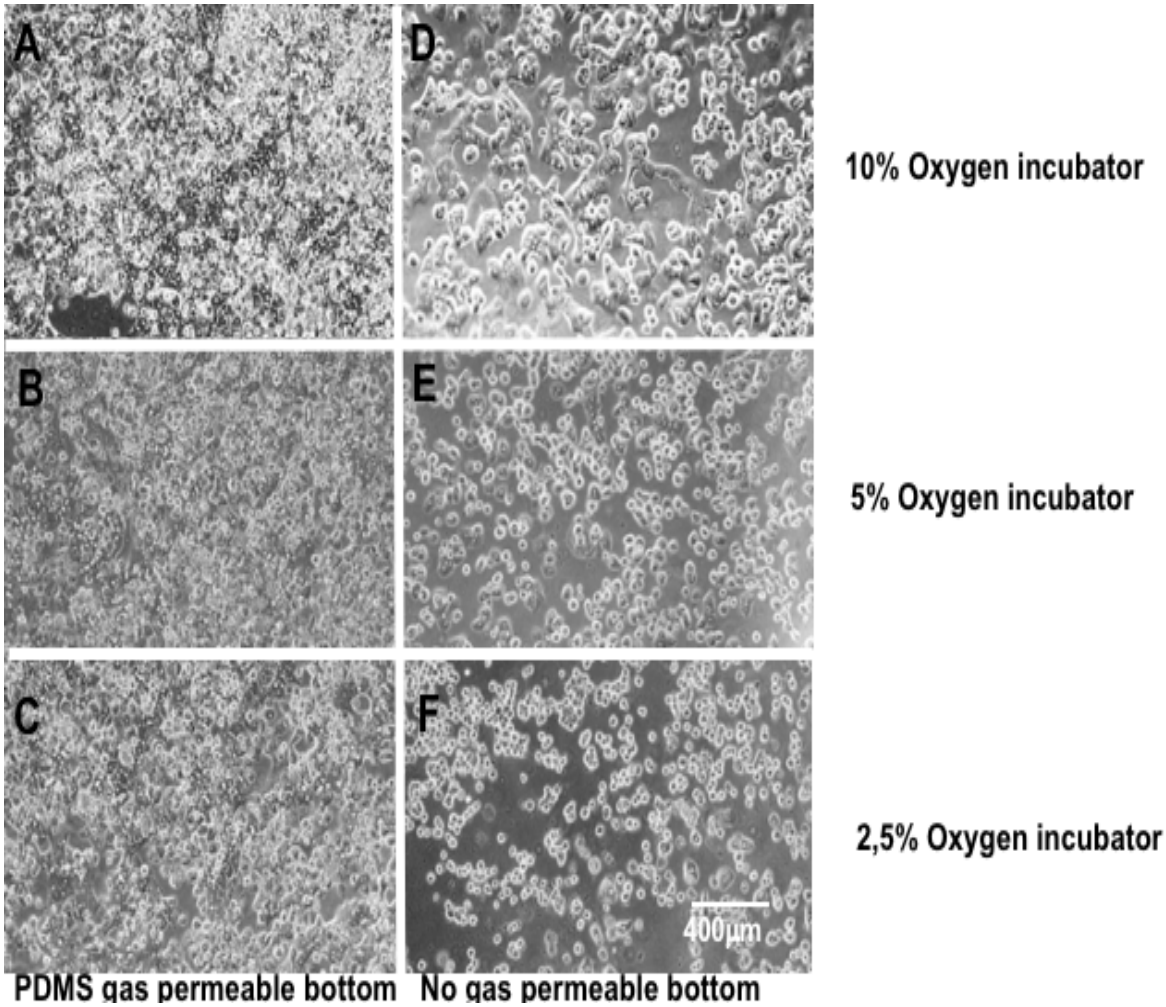


**Figure 3:** Morphologies of rat hepatocytes (A, B, C) PDMS plates (gas permeable bottom) after 24h of adhesion in 10; 5 and 2,5 % $O_2$ oxygen incubators; (D, E, F) polystyrene plates (no gas permeable bottom) cultures after 24h of adhesion in 10; 5 and 2,5 % $O_2$ oxygen incubators

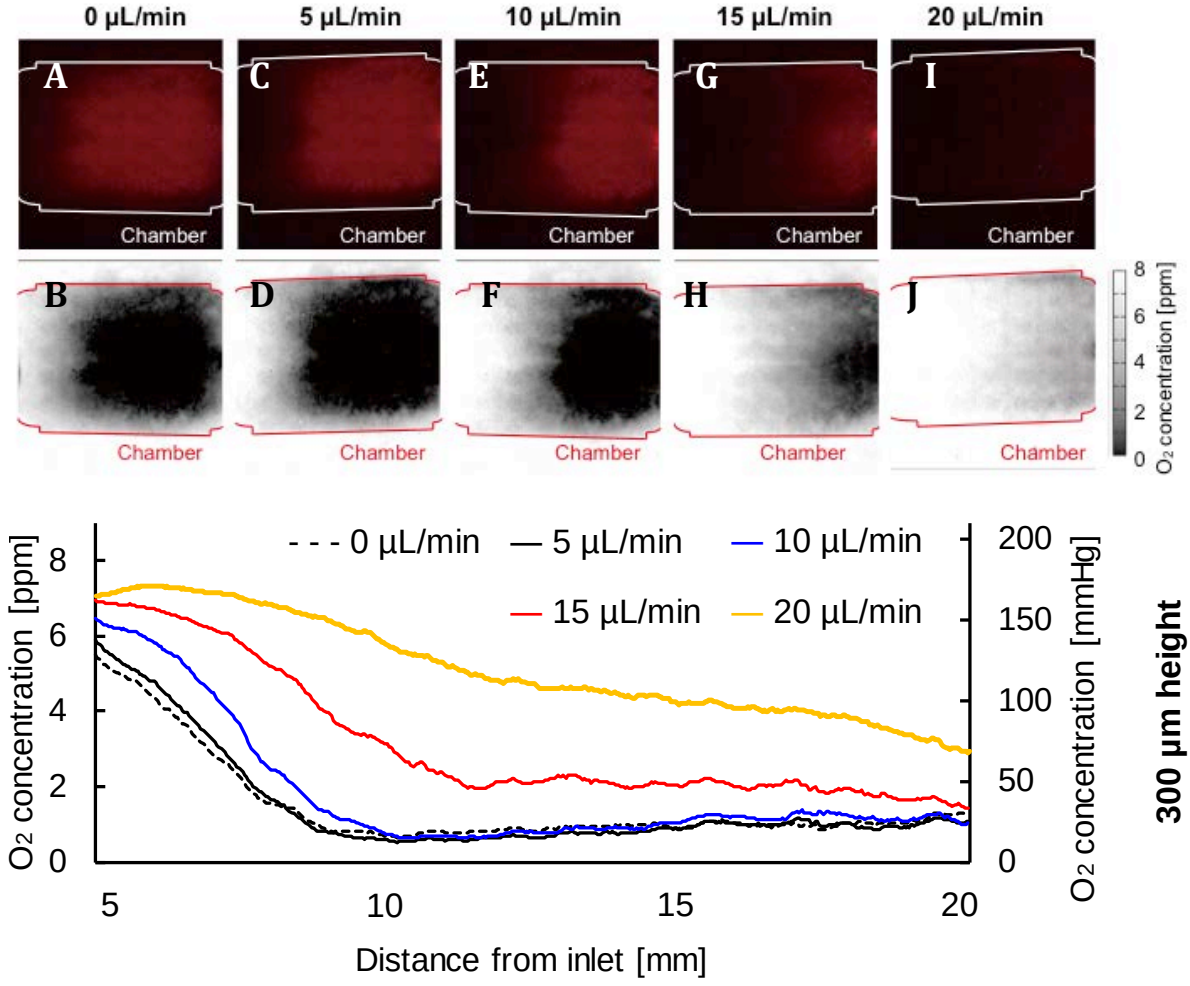

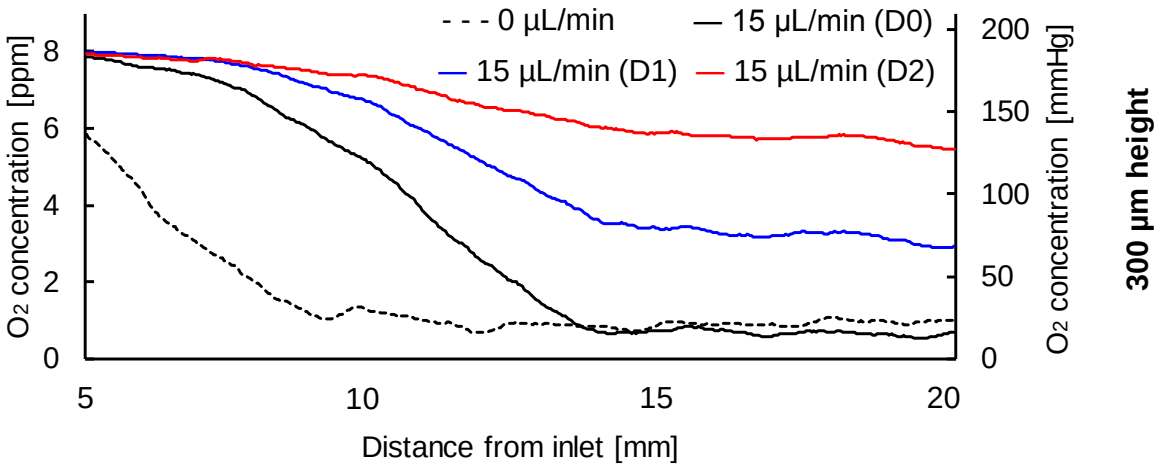


**Figure 4:** Fluorescent images of the PtOEP containing the oxygen sensor layer after 3h of adhesion (A) and 3h of adhesion + 30min of perfusion for 5, 10, 15 and 20 µL/min (C, E, G, I) and the 2D Profile extracted from the fluorescent conversion (B, D, F, H, J) using the Volmer equation and the image processing treatment (image processing is described in Matsumoto et al., 2018); (K) Central profile of the oxygen gradient along the longitudinal axis of the biochips at various flow rates after the 3h of adhesion and 30 min of perfusion; (L) at 15µL/min rate after the 3h of adhesion at rest, 30min (D0) 24h of perfusion (D1) and 48h of perfusion (D2) .

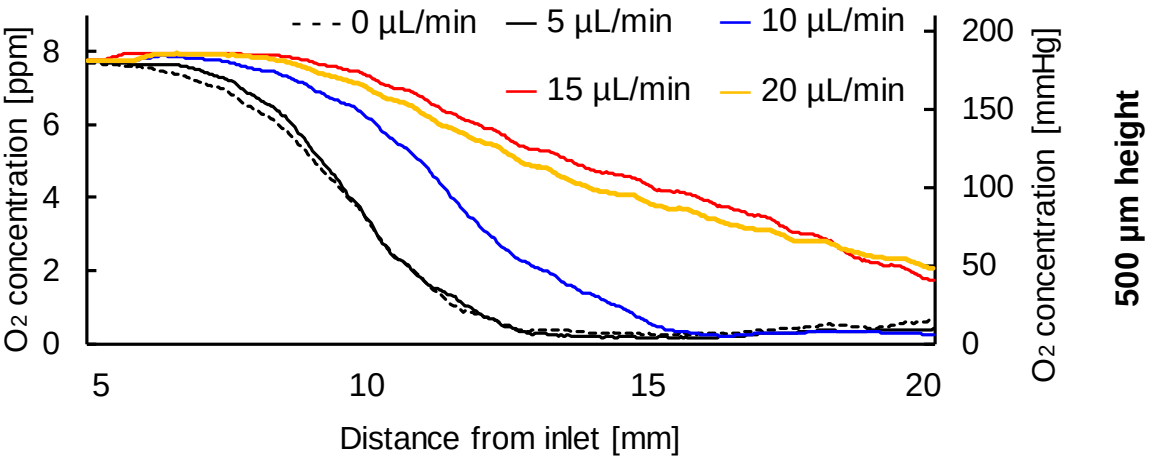


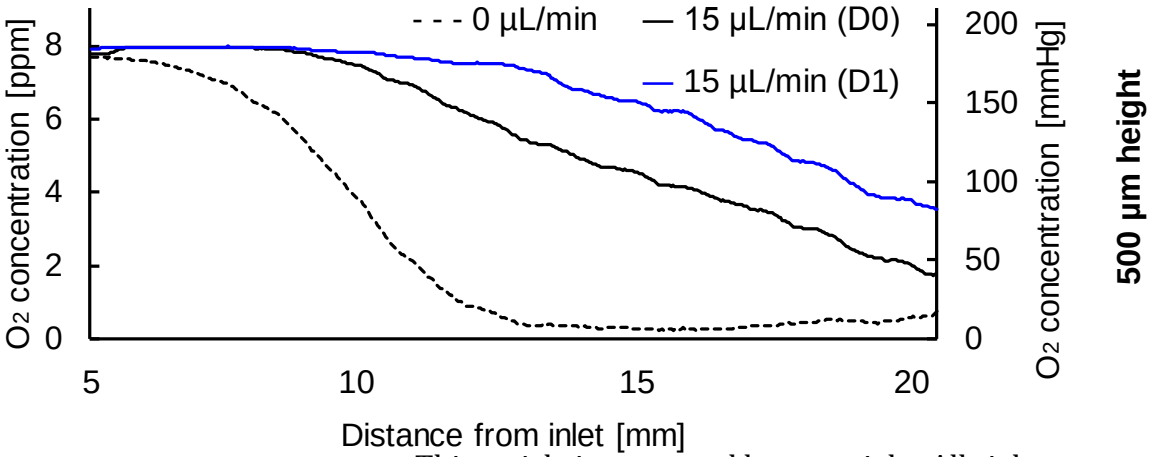

**Figure 5:** Central profile of the oxygen gradient along the longitudinal axis of the biochips (A) for 500 μm height culture device and various flow rates after the 3h of adhesion and 30min of perfusion (B) at 15μL/min rate after the 3h of adhesion at rest, 30min of perfusion 30min (D0) and 24h of perfusion (D1) .

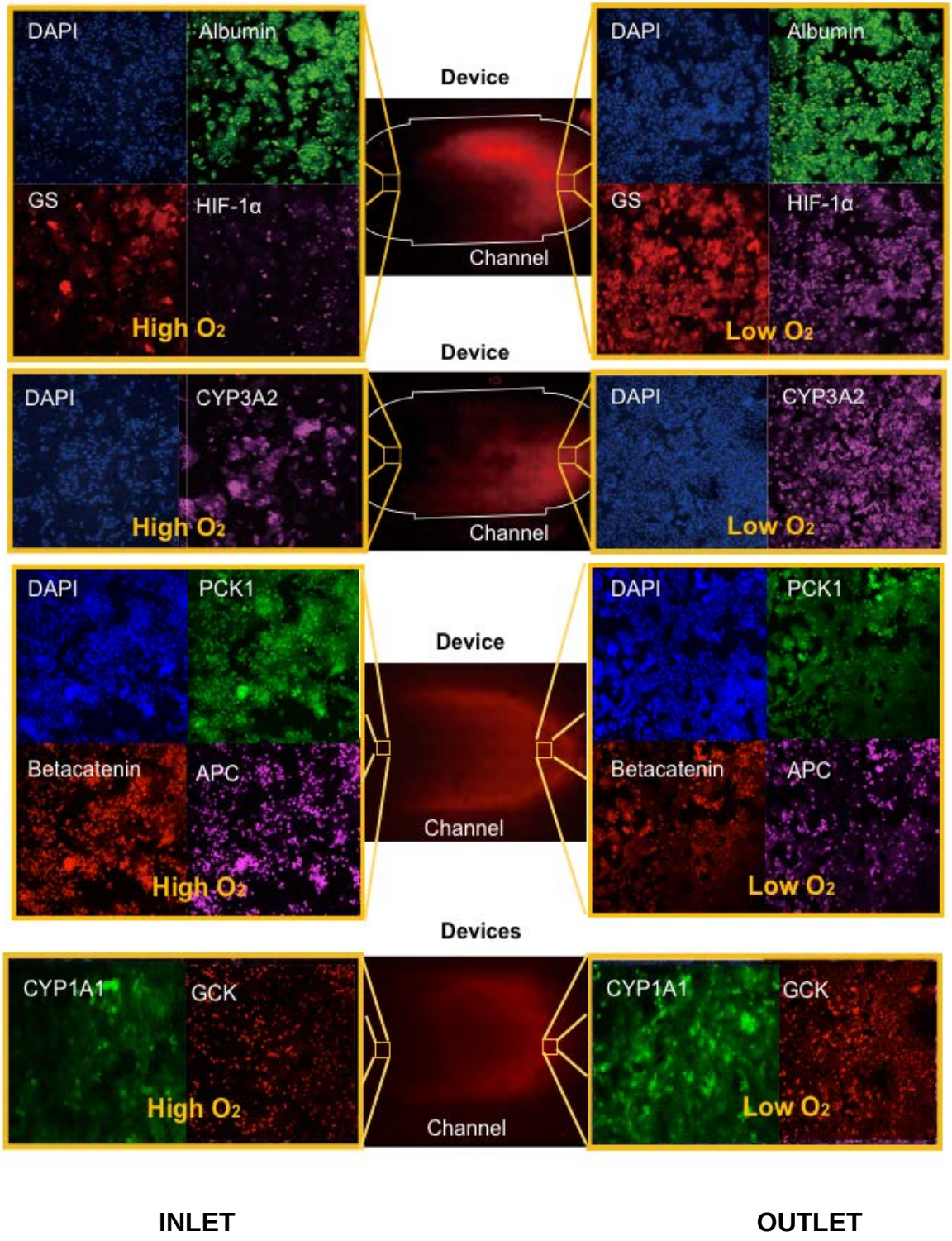


**Figure 6:** Fluorescent images of liver proteins immunostaining in the devices after 3h of adhesion followed by 24h of perfusion. Comparison of inlet versus outlet levels of

albumin, GS, HIFα, CYP3A2, ; PCK1, Betacatenin and APC and of CYP1A1 and GCK

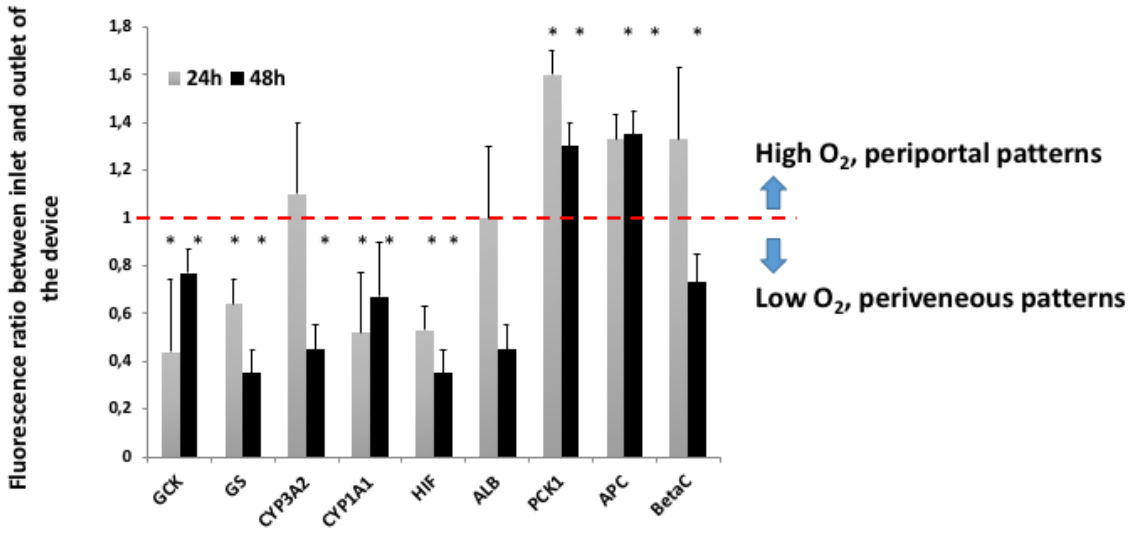


**Figure 7:** Fluorescent images processing comparing the inlet and outlet levels of fluorescence intensity inside the biochips. Data are normalised by the DAPI images. * reflects risk factor equality below 5% (comparison between inlet and outlet levels).

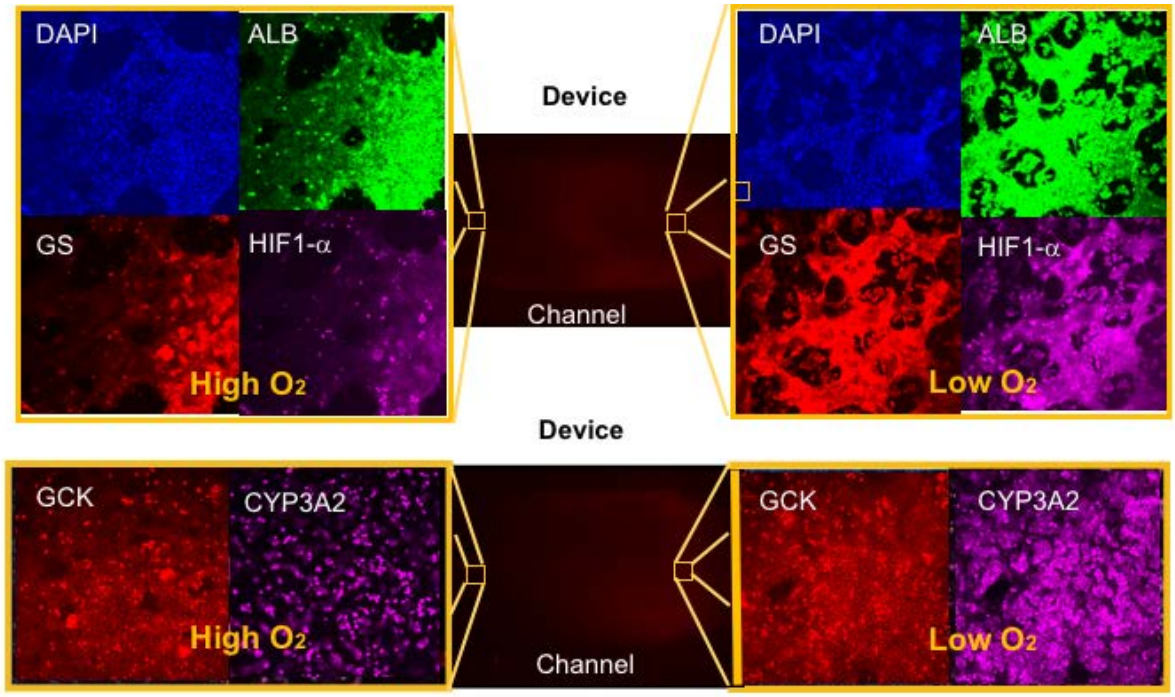


INLET
OUTLET

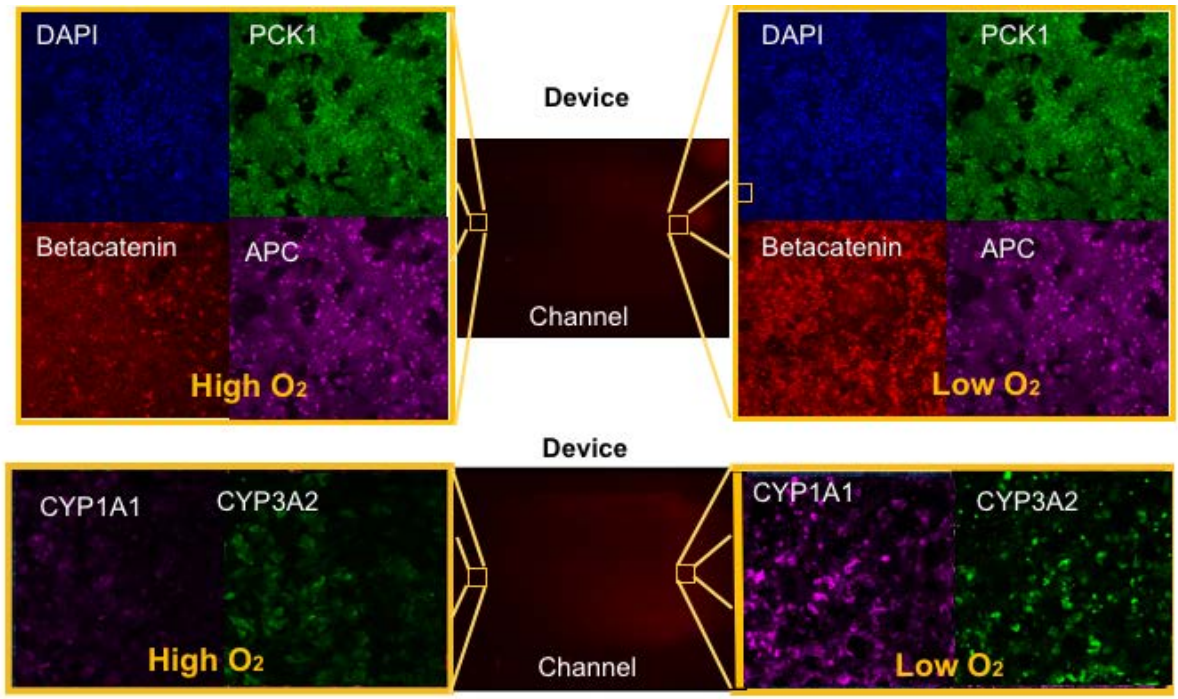


**Figure 8:** Fluorescent images of liver proteins immunostaining in the devices after 3h of adhesion followed by 48h of perfusion. Comparison of inlet versus outlet levels of albumin, GS, HIF$\alpha$; CYP3A2 and GCK; PCK1, Betacatenin and APC and CYP1A1